A study on Optical and Plasmon based trapping:

Towards Structured Light Fields

IISER PUNE

Thesis submitted towards fulfillment of

BS-MS Dual Degree Programme

by

SHREYASH TANDON

20091015

Under the guidance of

Dr. G V PAVAN KUMAR

Assistant Professor

Indian Institute of Science Education and Research, Pune

CERTIFICATE

This is to certify that the thesis titled "A study of Optical and Plasmon based trapping: Towards Structured Light Fields" submitted towards the fulfillment of BS-MS Dual Degree Programme of Indian Institute of Science Education and Research(IISER), Pune presents original research work carried out by SHREYASH TANDON under the supervision of Dr. G V PAVAN KUMAR at Indian Institute of Science Education and Research, Pune during the academic year 2013-2014.

SHREYASH TANDON   Dr. G V PAVAN KUMAR

    20091015   Assistant Professor

Acknowledgement

ABSTRACT

We have studied various aspects of development as well as applications of Optical traps. Design considerations of single beam optical traps and holographic optical traps using computer-controlled spatial light modulators(SLM) have been discussed and dealt with in this work. We predominantly use a 633nm He-Ne laser to trap 3-5 µm silica beads in various configurations. An introduction to structured light fields and in-depth studies of creation and properties of Bessel beams has been done. An SLM can be used to project holograms on its display which can alter both the amplitude and phase of incident light. This results into tailored light fields of different kinds. We have also demonstrated plasmonic trapping based on localized surface plasmons on a gold film coated glass slide. The evanescent mode of a 1064nm laser couples effectively at SPP resonance angle due to total internal reflection geometry of a dove prism. This leads to excitation of surface plasmon polaritons(SPP) on the gold film and formation of aggregates of 3µm silica beads which get trapped in this plasmonic potential well. Mobility of such aggregates with the movement of the incident laser spot has also been shown. Further, plans of using structured light fields(e.g. Bessel beams) in such experiments are discussed.

CONTENTS

Chapter 1

INTRODUCTION

1.1 History of Light-Matter Interactions

In the beginning of the twentieth century, a new wave of understanding in the field of electromagnetism affirmed it's rise. Landmark studies by Planck, Einstein and Compton showed that light was quantized and possessed momentum. Experimental researchers concluded[1,2] that transfer of momentum from photons to matter could result in physical motion. Such key studies brought forward an interesting and surprising concept : particles could be manipulated using the force exerted by light on matter. This force which is extremely small (order of piconewtons) on a macroscopic scale, is definitely not negligible at mesoscopic scale of cells and atoms. These developments are, what led Arthur Ashkin to his seminal work[3] in the field of trapping single particles using gradient force. They will be discussed at lengths later in this thesis, and these historic advances are what that gives direction to our work.

1.2 Motivation for the work

The idea of using momentum and force exerted by the light has come along way since its inception around four decades ago. Optical forces have been put to use in fields as varied as manipulation at micro and nano scales, atom optics etc. The introduction of structured light fields even widens the picture. In spite of these dynamic developments, this area of research has a lot to offer as many key questions remain unanswered. The idea of being able to localize light fields beyond the diffraction limit and observe its interactions with matter at small scale is extremely fascinating. To handle these advanced problems one has to venture into the field in an organized manner. Only if we get insights into the basics of these optical trapping and structured fields setups and design considerations, we can come up with new experiments to test interesting properties and applications. This forms the base motivation for this work. We tried to get hands on experience in this area so as to probe further advanced scenarios. An understanding and knowledge of how light behaves at small scales in the presence of matter is the goal that drives this research.

1.3 Plasmons

The interaction of light with metals, which forms a huge part of light-matter interactions gained understanding and pace with the discovery of plasmons. In the 1950s, oscillations of electron densities in plasma was observed for the first time. This phenomenon was tested and analyzed in various experiments using high energy electrons[4,5,6] which were bombarded on the plasma. It was observed that the patterns in the energy loss spectrum indicate the presence of these oscillations. Later, these oscillations were found to be not only confined to the bulk plasma, but also on the metal surfaces. R.H. Ritchie[7], in his experiments with a thin metal film bombarded by electrons predicted this phenomena. Subsequently, a series of experiments were done to characterize them, and the quanta of such collective surface oscillations were termed surface plasmons.

A unique property is the tendency of plasmons to get coupled with photons and form Surface Plasmon Polaritons (SPP) which can propagate along the metal-dielectric interface. This has led to propagation of light in sub-wavelength dimensions, beyond the diffraction limit[8]. This property has been extensively put to use in transferring information and sensing applications with a variety of sub-wavelength structures (e.g. nanowires, nanoribbons, chains of nanoparticles etc.)[9,10,11,12]. Another variety of Localized Surface Plasmons (LSP) have been used in molecular analysis up to single levels using Surface Enhaced Raman Spectroscopy(SERS) techniques.

1.3.1 Physical and Mathematical background

Now, with these two realms of light-matter interaction it is important to note that there is a significant amount of physical and mathematical background behind them. So we will leave the physics related to the trapping phenomena for later individual chapters, and go on here with the physics behind surface plasmons.

When we apply an electromagnetic field, the sea of electrons in a metal (according to the Plasma model) oscillate in response and their motion gets damped by a characteristic collision frequency, say $\gamma = 1/\tau$. τ is the relaxation time of the free electron of the order of 10^{-14} , so the frequency $\gamma = 100$ THz. If we assume that applied electromagnetic field has a harmonic time dependence, $E(t) = E_0 exp(-i\omega t)$ and solve the equation of motion of an electron

$$m\ddot{x} + m\gamma\dot{x} = -eE \qquad , \text{then}$$

$$X(t) = X(0)\exp(-i\omega t).$$

$$X(t) = \frac{eE(t)}{m(\omega^2 - i\gamma\omega)}$$

Where $\qquad X(0) = \dfrac{e}{m(\omega^2 - i\gamma\omega)}$

So, macroscopic polarization due to the displaced electron

$$P = -nex$$

$$P = \frac{ne^2 E(t)}{m(\omega^2 - i\gamma\omega)}$$

Consequently, the displacement,

$$D = \varepsilon_0 E + P \qquad\qquad \text{becomes}$$

$$D = \varepsilon_0 E(t) - \frac{ne^2 E(t)}{m(\omega^2 - i\gamma\omega)}$$

This can be further simplified to

$$D = \varepsilon_0 E(t)\left[1 - \frac{\omega_p^2}{(\omega^2 - i\gamma\omega)}\right]$$

where, $\qquad \omega_p^2 = \dfrac{ne^2}{m\varepsilon_0}$

This ω_p is called the plasma frequency of bulk plasmons.

Working towards the dielectric function of the given medium i.e

$$\varepsilon(\omega) = 1 - \frac{\omega_p^2}{(\omega^2 - i\gamma\omega)}$$

If we illuminate the metal-dielectric interface then the generated surface wave will propagate along the interface, but with an evanescent decay in the direction perpendicular to the interface. These waves bound to the surface and their quanta are termed Surface Plasmon Polaritons (SPP). The bulk Plasmon frequency and the surface plasmon frequency are related by :

$$\omega_{sp} = \frac{\omega_p}{\sqrt{1 + \varepsilon_2}}$$

where ε_2 is the dielectric permeability of the medium[13].

When the surface of the metal is illuminated two fundamental modes (m = 0,1) are excited. If the incident light is parallel polarized then m = 0 mode is excited and if the incident light is perpendicular polarized the m = 1 is excited. At any arbitrary polarization the net charge distribution at the surface is a superimposition of both these excited and propagating modes. These excitation modes tend to get damped over a distance because of losses due to surface roughness, coupling efficiency[14] etc. The resulting intensity can be calculated using the Propagation Length (L_0) which is the length at which the intensity of the SPP is 1/e times its initial value. Therefore, intensity

$$I(x) = I_0 \exp\left(-\frac{x}{L_0}\right)$$

From this, $\qquad L_0 = x/\exp\left(\frac{I_0}{I(x)}\right)$

Hence, the propagation loss (ß)[15] becomes

$$ß = -10 \log\left(\frac{1}{e}\right)/L_0$$

Even though these losses are quite inevitable, studies have shown that certain materials such as gold and silver have a property of sustaining these oscillations over a longer propagation distance. Waveguides(e.g. nanowires) made out of these materials have been shown to propagate SPPs up to lengths of tens of microns with significantly low losses[16,17,18,19].

In the next chapter, we will discuss the basics of Optical Trapping which will form the first realm of discussion for this thesis. We will look into aspects of setting up various kinds of optical traps and their properties and benefits.

Chapter 2

OPTICAL TRAPPING

2.1 Overview

During early 1970s Arthur Ashkin ushered the era of laser-based optical trapping. His observation, which he put forward in his number of seminal papers[3,20], of the capability of optical forces to displace and manipulate micron-sized dielectric particles in media like air and water was pioneering in this field. He was able to build a stable, three-dimensional trap based on counter-propagating laser beams. This later led to the development of single-beam traps using gradient force as the stabilizing factor, which are commonly referred to as 'optical tweezers' today[21,22]. Nowadays optical traps find varied applications in different realms of science. The ability to accurately apply and measure forces on the scale of piconewtons(pN) to micron-sized particles is being used to study systems like molecular motors in biology. Various modifications of simple optical traps are also being used to study colloidal and mesoscopic systems in physics and polymeric systems in chemistry.

2.2 Principles of Optical Trapping

An optical trap can be simply modeled as a microscopic simple harmonic oscillator. A dielectric particle near a focused beam produced using a high numerical aperture(NA) objective lens experiences two kinds of forces :
(1) A scattering force in the direction of propagation of light
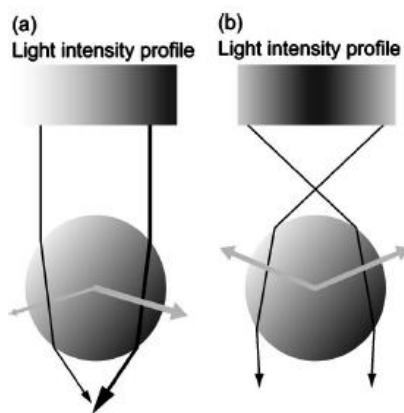(2) A gradient force in the direction of spatial light gradient

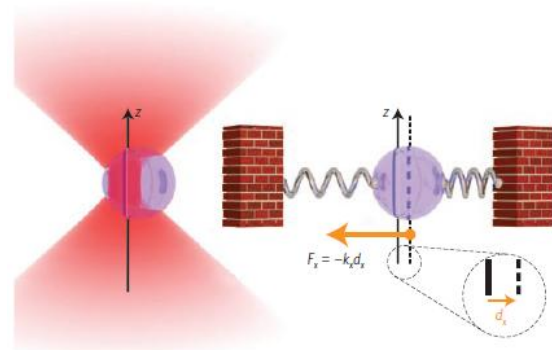**Fig 1 : Force diagram of gradient force near the focus [17]**

Fig 2 : Analogy with a simple harmonic oscillator [18]

The scattering force is due to the transfer of momentum of the photons impinging on the particle. This force tries to push the particle away from the focus and is the dominating one in most cases. The gradient force however depends on the intensity profile of the incident light and the polarizability of the particle. As we can see in figure 1(a), a beam of light which has a normal intensity gradient produces a gradient force which is towards one side and fails to balance the scattering force. But a focused light beam[fig 1(b)] produces a steep and radial intensity gradient that gives rise to a net upward gradient force which balances the forward scattering force. This balance is responsible for the equilibrium position of the trap being slightly off the focal point. This optical trap, at low displacements(~150nm) behaves like a Hookean spring whose force constant is proportional to the intensity gradient. Even though this explanation stays valid when the size of the trapped particle is much larger than the wavelength($a \gg \lambda$), the realm where Mie theory for scattering applies.

For particles of size much smaller than the trapping wavelength($a \ll \lambda$), we enter into the Raleigh scattering regime. Scaterring force is due to absorption and reradiation by the particle which is now treated as a point dipole. For a sphere of radius a,

$$F_{scatt} = \frac{I_0 \sigma n_m}{c}$$

$$\sigma = \frac{128\,\pi^5 a^6}{3\lambda^4}\left(\frac{m^2 - 1}{m^2 + 2}\right)^2$$

Here, I_0 is the incident light intensity, c is the speed of light, λ is the laser wavelength, n_m is the medium's refractive index and m is the ratio of refractive indices of the particle and the medium. The gradient force on the other hand is due to the interaction of the inhomogeneous field with the induced dipole

$$F_{grad} = \frac{2\pi\alpha}{cn_m^2}\nabla I_0$$

$$\text{where } \alpha = n_m^2 a^3 \left(\frac{m^2-1}{m^2+2}\right)$$

is the polarizability of the particle. When $m > 1$, the gradient force points upwards.

These underlying considerations for optical traps can be subtly tweaked to produce a variety of modifications in the nature and applications of this field. In this background, we will now move on the experiments in our lab where we realize some of these optical traps.

2.3 Single Beam Gradient Trap

In our very first experiment we experimentally realize the formation of a single beam gradient trap. The objective is to trap a single particle (here, a 5µm Silica bead) in a three-dimensionally stable optical trap.

2.3.1 Setup

Fig 3 : A schematic of the single beam gradient trap setup. M1,M2-mirrors; M3,M4-periscope assembly; L1,L2-beam expansion; BS1,BS2-beam splitters
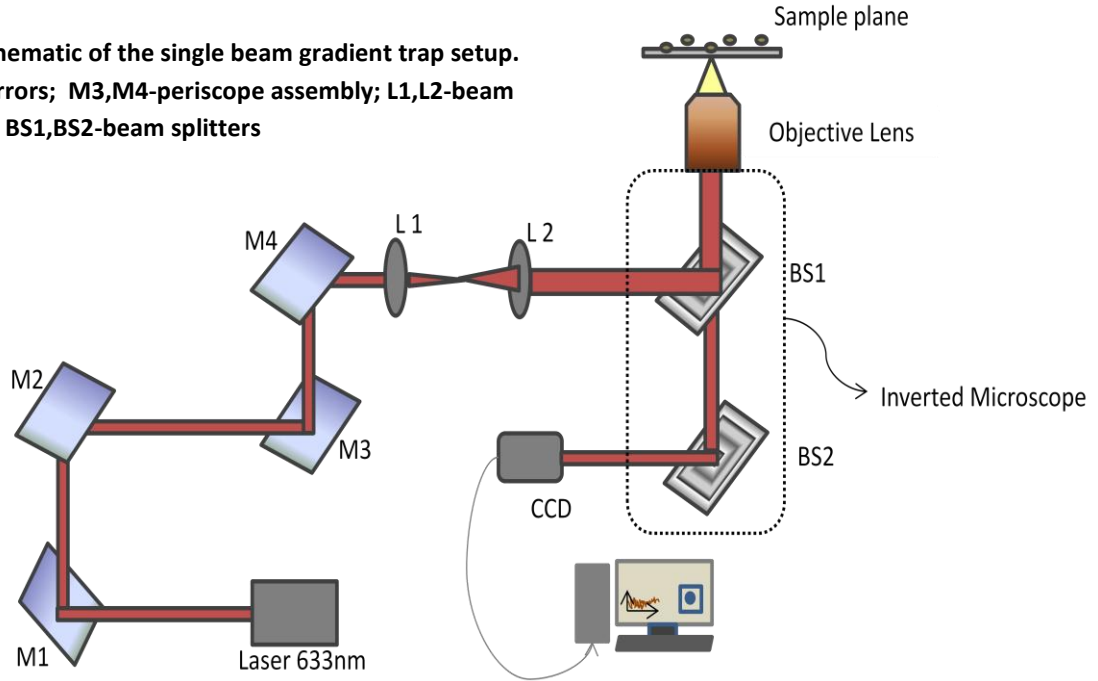
We use a 633nm He-Ne laser to trap the silica beads. The diameter of the bead is ~5µm and we use water as the medium in which the beads are suspended. The laser is steered using the mirrors and the periscope assembly into one of the ports of a commercial inverted microscope(Olympus IX371) setup. The lenses are for expanding the beam to overfill the objective aperture. This results in more efficient trapping since the external rays contribute disproportionally to the axial gradient force. The central rays, on the other hand, are primarily responsible for the forward scattering force. We use a high numerical aperture(NA=1.3), oil immersion objective lens(Nikon UPLAN FL; 100x). Note that the same objective is used for trapping and collection of the back-scattered light which is incident on the charge coupled device(CCD) camera.

2.3.2 Results and Discussion

The high NA objective creates a very sharply focused beam which leads to an optical potential near the focus. Silica beads which are in constant Brownian motion tend to fall

into this potential well when they are near the focus. The sample is kept on a mobile stage so that one can control the point of incidence inside the sample chamber. The strength and robustness of the trap depends on the intensity of the incident light. Following images show a trapped silica bead :
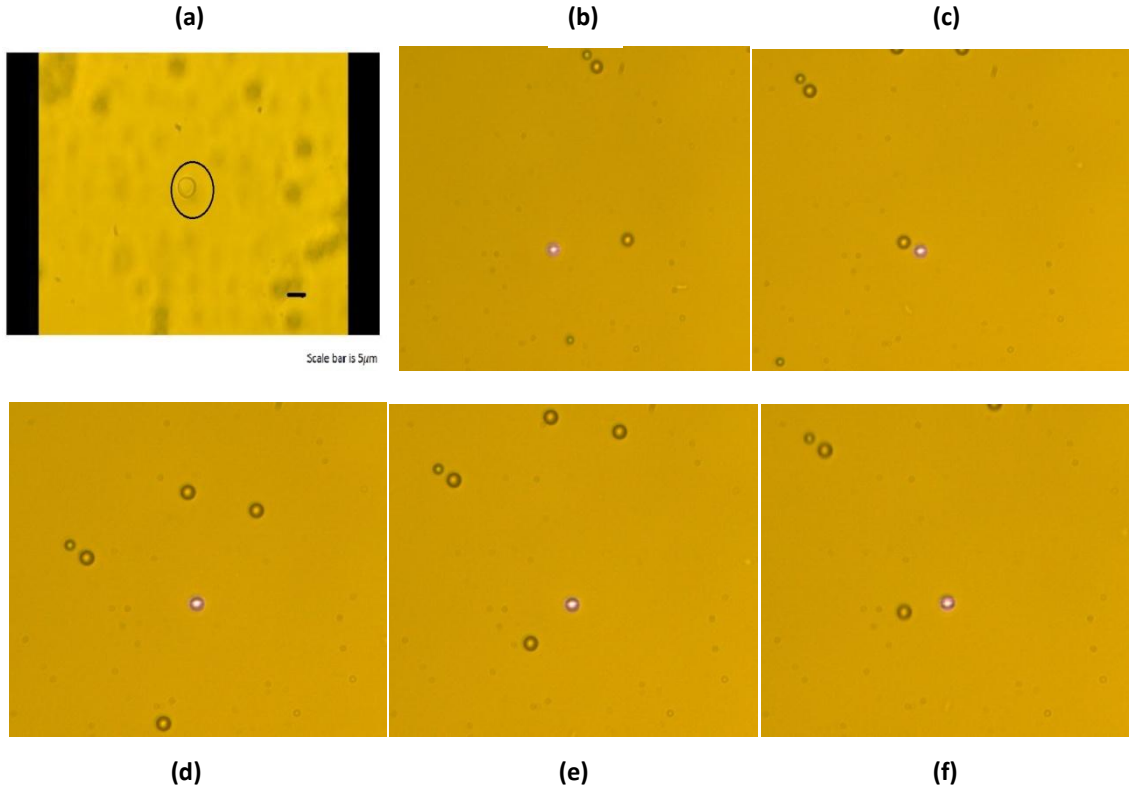
Fig 4: (a) trapped bead brought out in a different plane than other beads showing axial motion; (b),(c) motion along x-axis in the same plane; (d),(e),(f) motion along y-axis in the same plane

In figure 4(a), we see a single silica bead in a stable 3-dimensional optical trap. One of the advantages of the inverted setup is that the objective can be moved in the axial direction with the sample stage fixed. This enables us to move the trapped bead in axial direction. This is evident from the fact that all the other beads appear hazy except the trapped one which is brought into another plane using the mobility of the objective. In figures 4(b)(c), we introduce a drift of the fluid medium with respect to the trapped particle. This is done by moving the stage in the x-y plane so that the whole sample chamber moves. From the surroundings of the trapped bead in the images, we can see that the bead is held stationary even though the medium containing it is moving horizontally i.e along x-axis. A similar motion is performed for the vertical i.e. along y-axis as well. This confirms the stability of the trap in the x-y plane.

Thus in this experiment, we have come up with an optical trap which is stable in three dimensions and also demonstrated a technique to move about the trapped particle in both the plane of trapping and axially. This technique can also be used to measure the stiffness of the optical trap by doing force measurements. This has been widely done using quantum photo diodes(QPD). Such single beam gradient traps have been used for various colloidal systems, biological particles(e.g. bacterium), macromolecules and polymers in various applications.

2.4 Structured Light Fields

After having trapped a single particle the natural extension one thinks towards is trapping of multiple particles. Better still multiple independently controlled traps are the next step. Simpler modifications like two particle traps have been realized quite frequently using a pair of beam splitters and steerable mirrors[23]. Techniques like Acousto-Optic Deflectors(AOD) and rapidly scanning galvo-mirrors have also been used to create multiple-particle traps[24,25,26] but they predominantly involve time-sharing of a single beam to create multiple traps. This renders simultaneous control and independent axial manipulations of the individual traps impossible.

In 2002, Curtis *et al.* came up with the concept of holographic optical tweezers. In their seminal paper they demonstrated the use of a commercially obtained spatial light modulator(SLM) as a diffractive optical element(DOE). This technique could split a single light beam into multiple independently controlled traps. These multiple beams could also be independently positioned in 3D and even the point-spread function of each could be controlled individually[27,28]. The following figure gives an example of a simple setup for a holographic trap

This was the earlier in a series of works which employed spatial light modulators in the field of optical trapping. We will now move on to some important aspects and advantages of these SLMs before discussing our own trapping experiment.
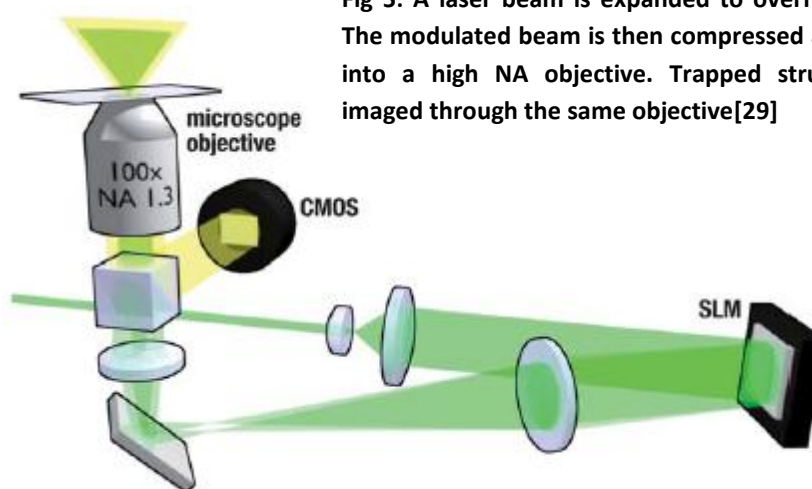

Fig 5: A laser beam is expanded to overfill the SLM. The modulated beam is then compressed and imaged into a high NA objective. Trapped structures are imaged through the same objective[29]

2.4.1 Spatial Light Modulators(SLM)

From being developed for use as devices for video projection, SLMs have come a long way in terms of their applications in not only optical tweezers but also in microscopy. These programmable devices have the capability to modify both the phase and amplitude of the light incident on them. The most widely used type of SLMs are just miniaturized liquid crystal displays(LCD). The high resolution of LC-SLMs gives the user to control upto 2 million pixels on a screen of about $2cm^2$.

Fig 6: Schematic of a parallel aligned LC cell. Changing voltage causes birefringent molecule to rotate along an axis perpendicular to both light propagation and the polarization vector[30]
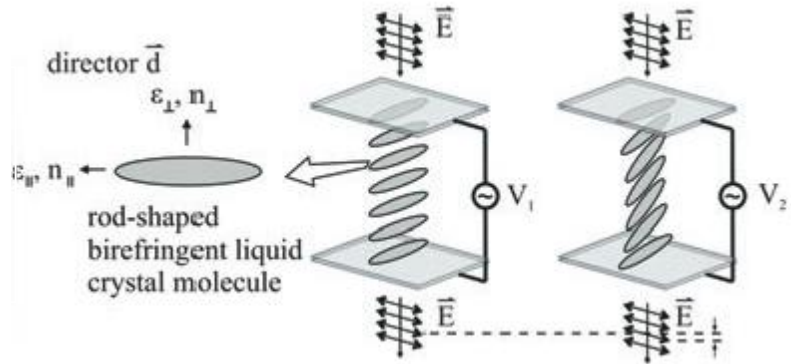
The birefringence of the liquid crystal is primarily responsible for both amplitude and phase modulations. Amplitude modulations which originate form polarization modulations can only be observed behind a polarizer whereas achievable phase modulations are only in the range of 2π. Even though higher phase dynamics can be generated by accordingly wrapped patterns.

SLMs have been used in various configurations at different points in the optical train. In the figure are some of the widely used configurations.
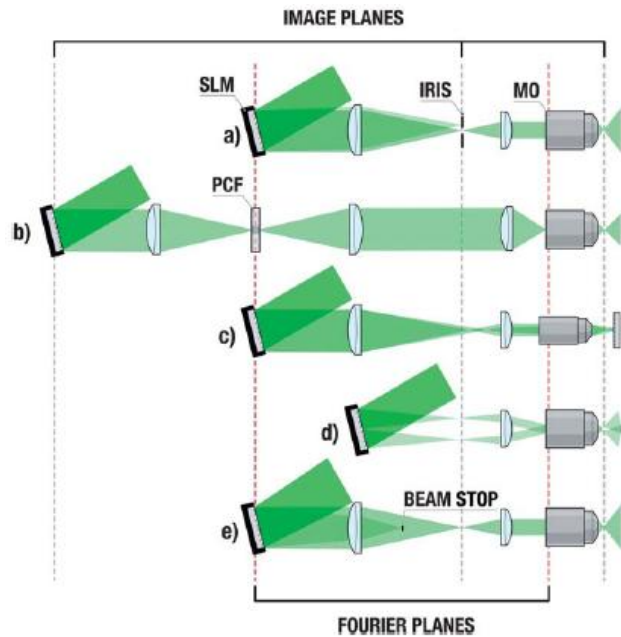
Fig 7: (a) SLM in the Fourier plane of the sample, (b) in the image plane using phase contrast approach, (c) mirror behind the sample plane to create counter-propagating beams for long working distance traps, (d) Fresnel plane (e) close to Fourier plane to filter the zero-order beam[29]

The SLM which we use in our lab for the following experiments is a Holoeye LC-R 2500. It has a resolution of 1024x768 with a pixel pitch of 19μm. With a 93% fill factor and a frame rate of 72 Hz, it gives a good response in visible(633nm) frequency range. Since we are talking about structured light fields, given below are some images as an example of how these beams look like. Please note that these are pre-stored holograms in the device but one can create desired patterns by creating computer generated holograms.
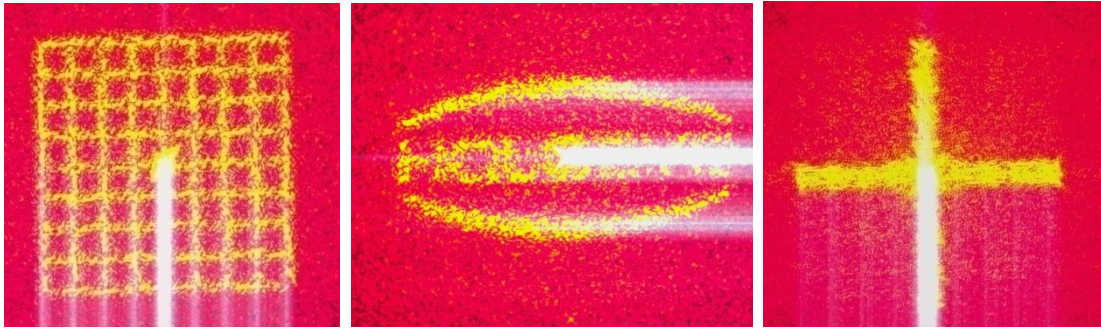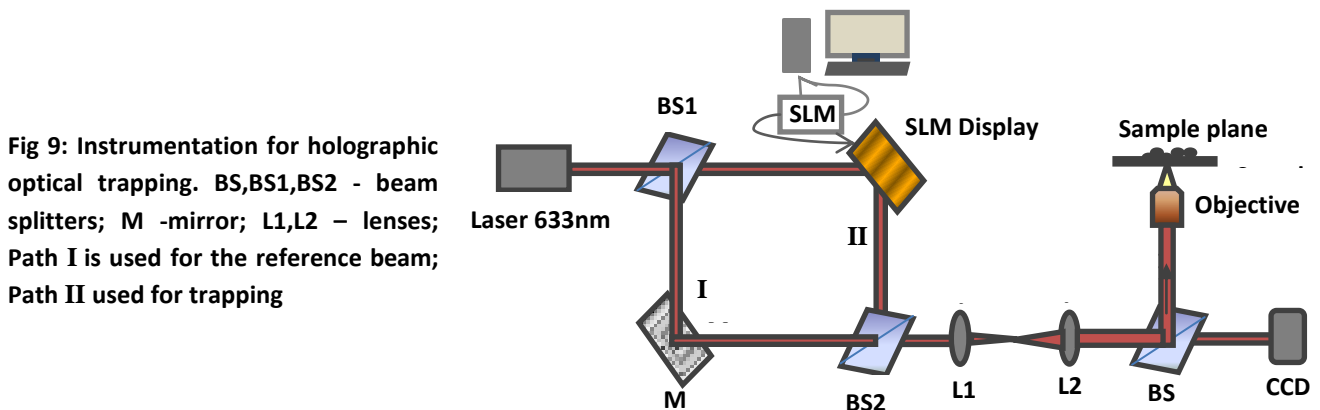

Fig 8: Some pre-stored holograms projected on a ccd. They show the variety of modulations possible

2.5 Holographic Optical Trap

The next step in line was to venture into trapping multiple particles using a modulated light field. The aim of this next experiment was demonstrating a stable trap of a few silica beads suspended in a medium.

2.5.1 Setup

We used the above mentioned(Holoeye LC-R 2500) SLM to project a pre-stored structured light beam into our inverted microscope(Olympus IX 371) setup. Incident light of 633nm wavelength was used for trapping and the focusing is done with a 100x, high numerical aperture(NA=1.3) objective(Nikon UPlan FLN). The setup for the experiment is as shown below :

Fig 9: Instrumentation for holographic optical trapping. BS,BS1,BS2 - beam splitters; M -mirror; L1,L2 – lenses; Path I is used for the reference beam; Path II used for trapping

The lenses L1, L2 form the usual beam expansion mechanism to overfill the objective aperture. An important thing to note are the two paths labeled as I and II, Path I is used as a reference to align the incoming beam properly whereas path II contains the SLM required for the holographic trap. Alternatively, if the SLM in this path is replaced by another steerable mirror, one can realize a two-particle trap with individual maneuverability. The size of the silica beads used is again ~5µm.

2.5.2 Results and Discussion

Once the optical train is aligned properly we block the path I and allow light only through path II to enter the objective. Imaging is done through the CCD camera attached one of the exit ports of the microscope. Holograms displayed on the SLM are faithfully projected on the sample plane creating structured potentials. Silica beads, which otherwise are in random Brownian motion fall into these array of optical potentials created and exhibit a stable trap. Images of some traps are shown below:
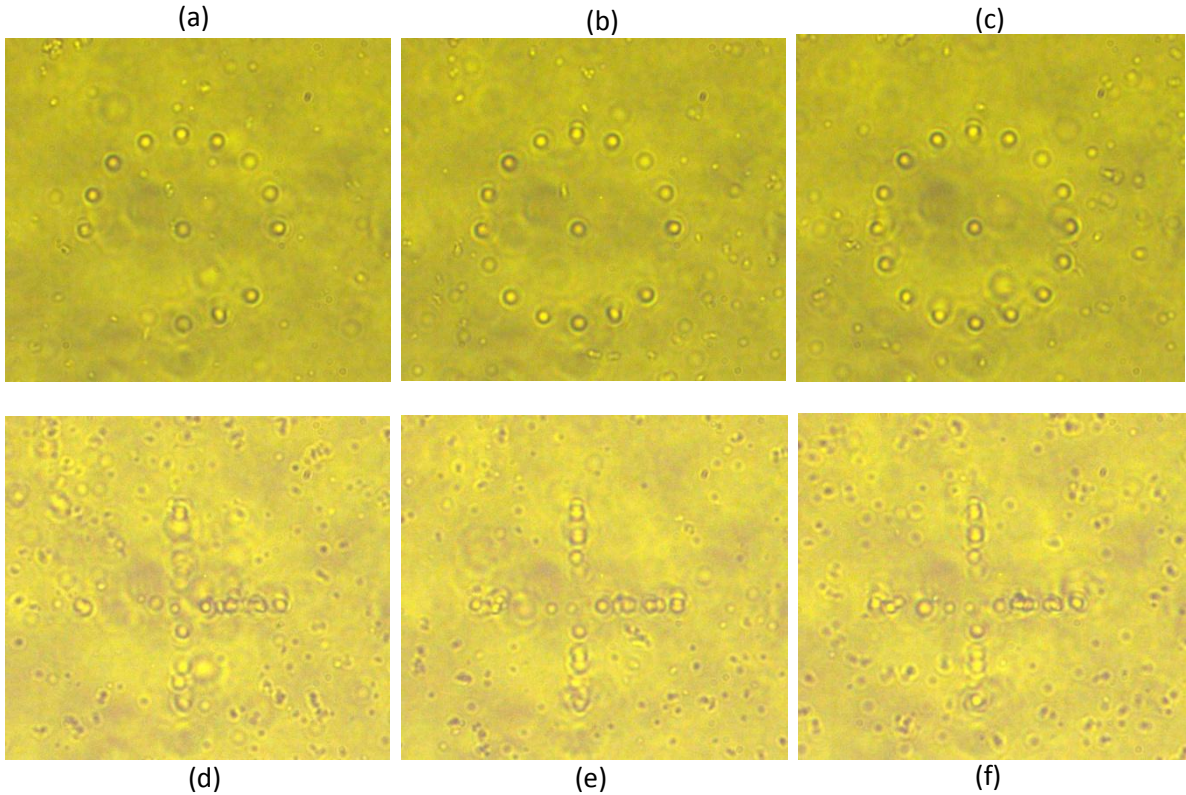
Fig 10: (a,b,c) beads come in and out of a holographic trap forming a perfect trap eventually; (d,e,f) same phenomena for a different kind of modified light field

As we can see in the images, when a shaped light beam is incident all the beads don't get trapped into available potentials immediately. Some vacant spots are seen. But in a while

at least one bead is trapped in each optical potential well. A complete trap is seen in figures (c) and (f), whereas incomplete traps can be seen in other figures. Areas where the intensity of the incident light is slightly higher exhibit more stable and robust traps. This happens because the hologram displayed on the SLM display can't be perfectly projected in the sample plane resulting in loss of intensity in some areas. Still, these images confirm relatively stable holographic traps. Although these experiments were done with pre-stored holograms, one can use tailored modified fields as well by programming in the SLM.

After being able to realize such holographic trap the interest moves on to certain types of structured beams which possess special properties and applications. One of the very interesting beam geometries are the Bessel beams. They have a number of unique properties rendering them applicable in a wide variety of experiments. The next chapter will specially be dedicated to the study of these Bessel beams.

Chapter 3

BESSEL BEAMS

To any propagating beam of light(e.g. Gaussian beam) is linked the inherent phenomenon of diffraction. We believe the light coming out of a laser aperture to have very less divergence as it propagates but the diffraction causes light to spread over a given distance. In fact the Rayleigh range is a criterion to determine the spread of a beam and is defined as the distance in which a beam's cross-sectional area doubles. This distance is given by the equation

$$Z_R = \frac{\pi w_0^2}{\lambda}$$

where w_0 is the beam waist and λ is the wavelength of light. However there are some special light fields which are somewhat immune to this diffraction. Jim Durnin was the first to study Bessel type, propagation direction invariant solutions to the Helmholtz equation. He reported[31] that such beams could possess near diffraction limited properties. As expected the name comes from the cross-sectional profile of the beams which are described using Bessel functions. Now the problem was that Bessel beams can theoretically contain an infinite number of concentric rings. That means infinite power in a beam and hence it can't be realized in the laboratory. But, Durnin and group were able to demonstrate[32] quasi-Bessel beams which possess the theoretical properties over a finite distance. However they cautioned that any comparison with the Gaussian beam had to made with the central core of the Bessel beam which is non-diffracting and propagation invariant.

3.1 Generation techniques

3.1.1 Annular Slit approach

Durnin *et al.* used this technique for generation of Bessel beams. A review in *Contemporary Physics*[33] provides a decent schematic for this setup. They employed the fact that these beams can be safely assumed as the Fourier transform of a ring as is evident from
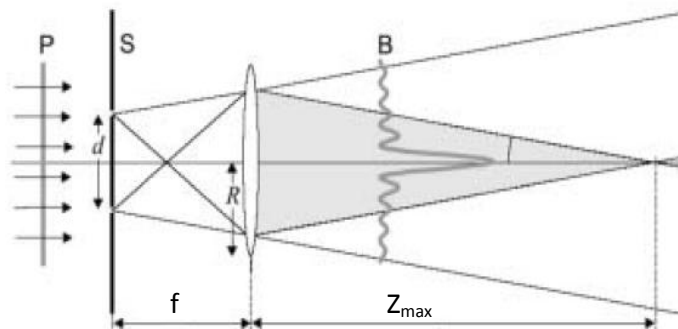

Fig 1: Schematic of the annular slit setup [33]

their angular spectrum. They placed an annular slit which acts like a ring in the back focal plane of a lens to form the beam. The propagation distance of this Bessel beam can be determined by the opening angle of the conical wavefront and is given by:

$$Z_{max} = \frac{R}{tan\theta}$$

where $\quad tan\theta = \frac{d}{2f}$

This method suffers from wide oscillations in the on-axis intensity of the beam and is very inefficient. The reason for that being obstruction of most of the incident power by the annular slit.

3.1.2 Axicon approach

Certain groups have used[34] axicons or conical lens elements to generate these beams. The figure illustrates this method of generation. In this case the opening angle of the conical wavefront is given by:
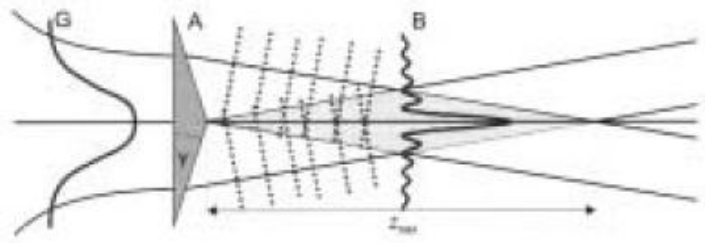

Fig 2: Schematic of the axicon setup[33]

$$\theta = (n-1)\gamma$$

where γ is the opening angle of the axicon and *n* is its refractive index. The propagation distance in this case can also be similarly calculated as in the last approach. The main advantage here is that we are using most of the Gaussian beam. This amounts to this method being more efficient and one observes smoother intensity variations rather than rapid on-axis variations in the last method.

3.1.3 Holographic techniques

In present day, the much more efficient method to generate these beams is by holographic means. The objective is to imprint the phase of the Bessel beam onto the incident Gaussian beam. This can either be done by static etched holograms or by using computer-controlled spatial light modulators(SLM). This is how we generate the Bessel beams in our laboratory. Durnin gave a general solution of the scalar wave equation for a non-diffracting beam of the form :

$$E(x',y',z' \geq 0,t) = \exp[i(\beta z' - \omega t)] * \int_0^{2\pi} A(\varphi) \exp[i\alpha(x' \cos\varphi + y' \sin\varphi)] \, d\varphi$$

where A(φ) is a complex amplitude function; (ρ,ϕ) are polar coordinates in the grating plane; (x',y') are coordinates in the image plane; z' is the distance between the grating and the image plane; and $\alpha^2 + \beta^2 = k^2$, with k being the wave number. Now if we have a hologram of radius R with an amplitude function[35]

$$t(\rho,\varphi) = A(\varphi)\exp\left[i\left(\frac{2\pi\rho}{\rho_0}\right)\right] \text{ when } \rho \leq R; \ t(\rho,\varphi) = 0 \text{ when } \rho > R ; \quad \alpha = \frac{2\pi}{\rho_0}$$

and we consider $A(\varphi) = \exp(in\varphi)$, then E(x',y',z',t) becomes a Bessel function of the first kind of order n. Further, t(ρ,ϕ) becomes a phase function of the form:

$$t(\rho,\varphi) = \exp[i\psi(\rho,\varphi)] \ \text{ where } \psi(\rho,\varphi) = n\varphi + 2\pi\rho/\rho_0.$$

If we code the Fourier transform of this phase function on a 3D plot in MATLAB we get a
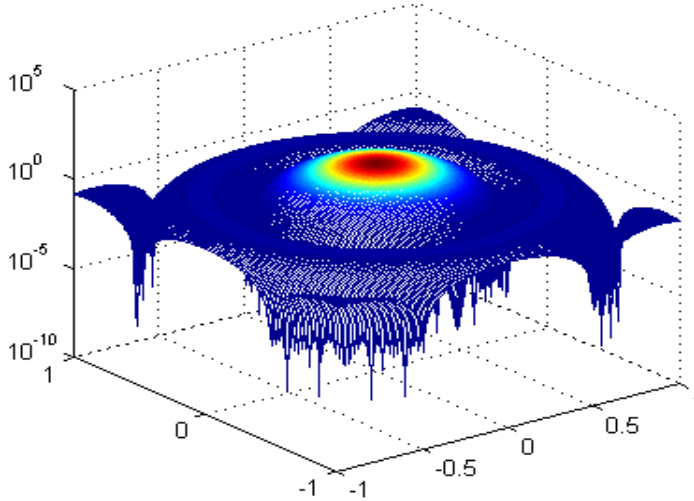
Fig 3: A MATLAB plot of the Bessel function type intensity pattern of the beam

good idea of the intensity distribution of the beam wavefront which is clearly similar to a Bessel function(figure 3).

This phase function in the form of axicon phase was displayed on a Holoeye L-CR 2500 SLM in our lab. This is a reflective type SLM a simple setup (figure 4) is shown. The beam expander(L1, L2) is to cover most of the hologram display area of the SLM so as to achieve a good resolution. Lens L3 focuses the image on the CCD.
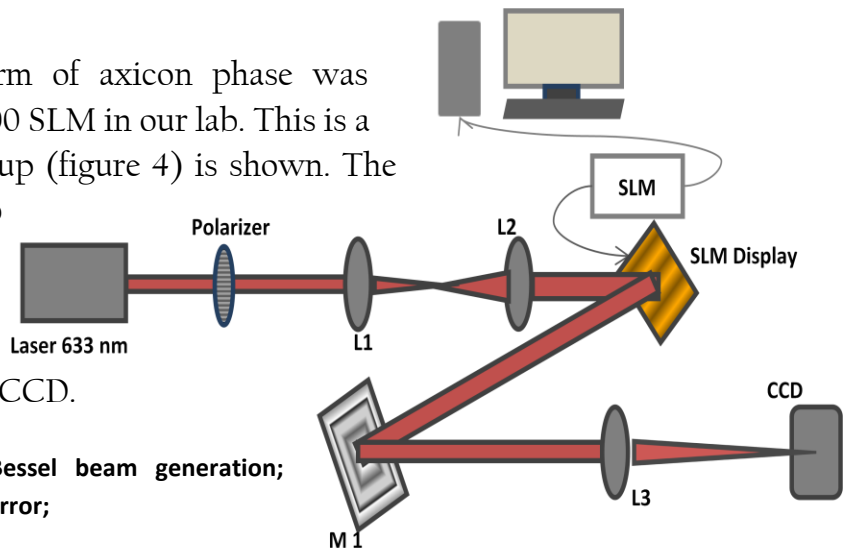
Fig 4: Setup for the Bessel beam generation; L1,L2,L3 – lenses; M1 – mirror;

22

Shown below are the images of the Bessel beams at different zoom values that we generated in our laboratory. It can be clearly seen that the number of rings in the field of view depends on the zoom value.

(a)   **(b)**   **(c)**   **(d)**
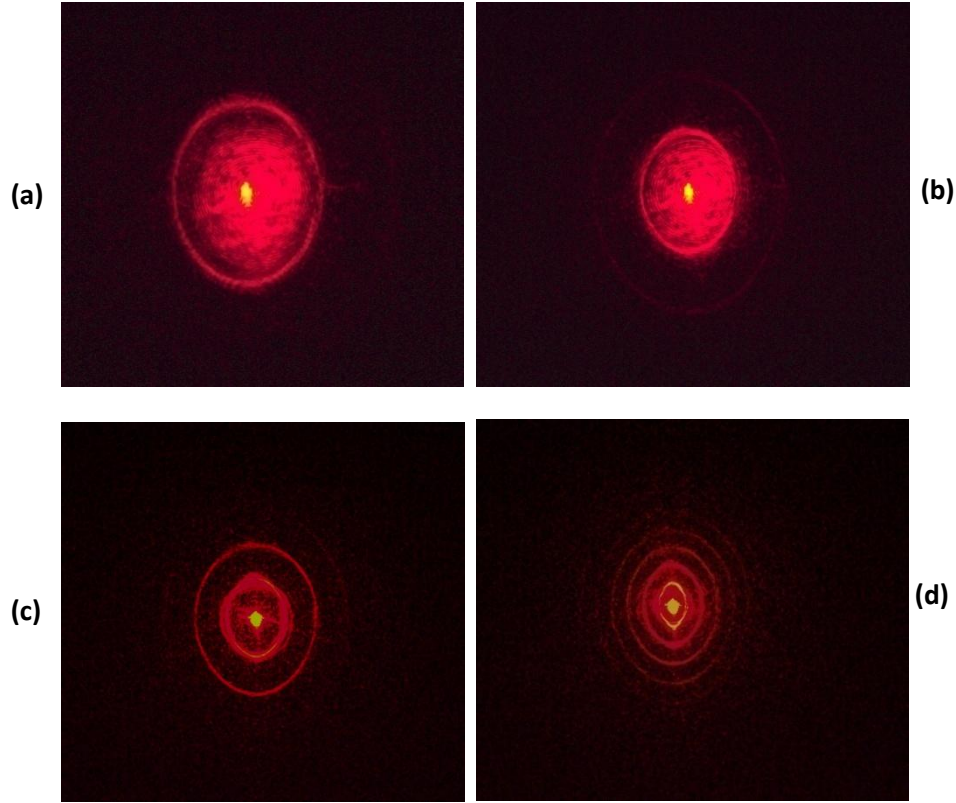
Fig 5: Bessel beams at different zoom values of the hologram; (a) 31%; (b) 40%; (c) 50%; (d) 100%

3.2   Properties and advantages

The fact that these are non-diffracting beams provides certain advantages specially in the field of optical manipulation. Although they don't have a specific focus to realize a genuine three-dimensional trap, the central core of this light fields is great to confine particles in two dimensions and move them axially over longer distances. Also the long and thin core is ideal for trapping elongated objects, for example, nanorods or bacteria like E-coli. The multiple ring structure is also proves to be useful as it gives the ability to trap low and high refractive index particles simultaneously by the same beam. The low index particles get trapped in the dark regions between the bright rings, whereas the high index particles get trapped in the rings itself.

Another property that these beams exhibit is the ability of self-reconstruction after an

obstacle in their path. Gaussian beam traps have good efficiency near the focal point but the optical forces are insufficient even a few microns away. Bessel beams, however due to conical wavefronts, can self-reconstruct their profile after trapping say one particle, and then go on to trap multiple particles along the same axis. This remarkable phenomenon combined with the usual radiation pressure has been put to use in creating wave guide like properties for single as well as multiple particles. The many ringed structure with varying intensities has also been used as a tilted washboard potential to amalgamate small microspheres over a large area towards the central beam.

Another area of specific interest has been the high-order Bessel beams(HOBBs). These have an intensity minima instead of a maxima at the centre and the rest of the profile is similar. The central core can therefore be used to confine low index particles or samples which are susceptible to damage due to incident light, e.g. biological specimens. They have also found numerous applications in the studies of orbital angular momentum carrying light fields. Such fields, for example, Laguerre-Gaussian modes can be used to rotate trapped particles by transfer of the angular momentum which has given a huge push to the field of microfluidics. These have also proved helpful in designing mechanical elements like motors, valves, channels etc. at micro or nanoscales. Other than these wonderful applications Bessel beams are now being used in the field of atom optics and non-linear optics regime.

In the next chapter we discuss about a different kind of trapping called plasmonic trapping and also how we plan to incorporate Bessel beams in such trapping experiments.

Chapter 4

PLASMONIC TRAPPING

4.1 Overview

The problems with optical trapping creep in once we reduce the size of the particles to be trapped to dimensions smaller than the wavelength of light. There are a couple of considerations which play a key role here. First, with decrease in size the magnitude of restoring force required to create a robust trap decreases rapidly. This results in a smaller potential well for the particle to sit into. Second, the damping due to viscous forces decreases a lot due to reduction in size. Both of these factors contribute to destabilizing an optical trap. The only solutions which present themselves i.e. further increasing the focusing of light(diffraction limited) and increasing the intensity of the incident light(harmful for the specimens) are rendered rather unviable.
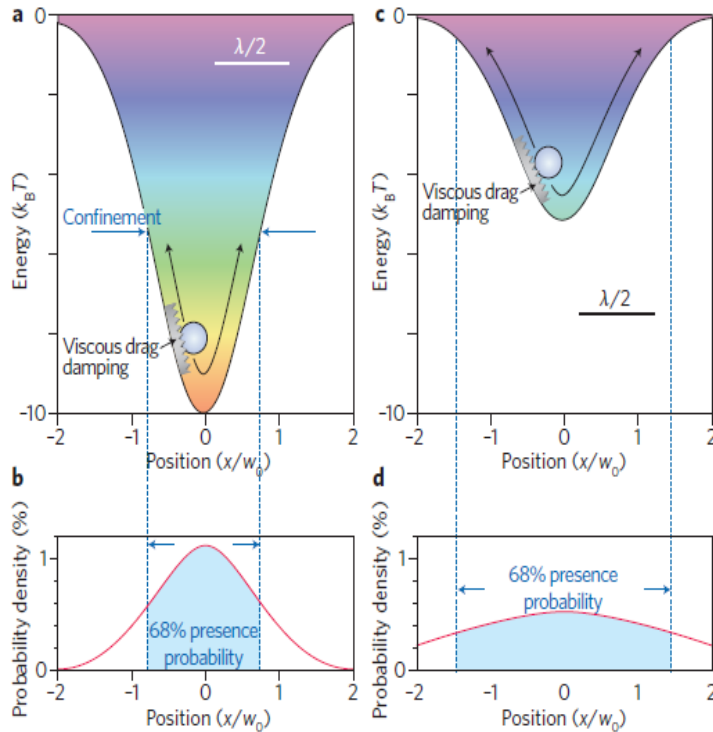

Fig 1: Conventional optical trapping vs Surface Plasmon trapping. [38]: (a,b) Trapping potential and associated position distribution of a polystyrene sphere; (c,d) same parameters for a 20% reduction in size; (e) Optical potential landscape in case of an illuminated gold nanostructure;Half wavelength bars are for a scale of reference

An alternative to go around these barriers involves the application of surface Plasmon resonances in optical trapping. Unlike propagating fields, evanescent fields are not diffraction-limited and can be localized to very small scales, even beyond the diffraction

limit. Engineered plasmonic nanostructures have been shown to efficiently couple propagating light fields and localize them into small and intense optical fields. These highly localized areas of intense fields are termed as "hot spots". The interaction of propagating light fields with these structures thus create large *k-vectors* characteristic of evanescent waves resulting in sub-wavelength localization. In other words, nanostructures act as some sort of 'plasmonic lens' to focus light at nanoscale. The work by Garces-Chavez *et al.* regarding assembly of dielectric beads on a gold substrate[36] and Volpe *et al.* regarding photonic force microscopy[37] were pioneering researches in this field.

4.2 Methodology

To achieve stable trapping using SPPs on a metal surface, one has to take into consideration the momentum matching problem. Since SPPs are pure evanescent modes they can't be coupled directly to propagating light fields. In order to overcome this total internal reflection from a prism surface to increase the wave number(and momentum) is used to excite these surface plasmons. One of the two configurations are invariably used for this purpose which are; a) Otto configuration , b) Kretschmann configuration.
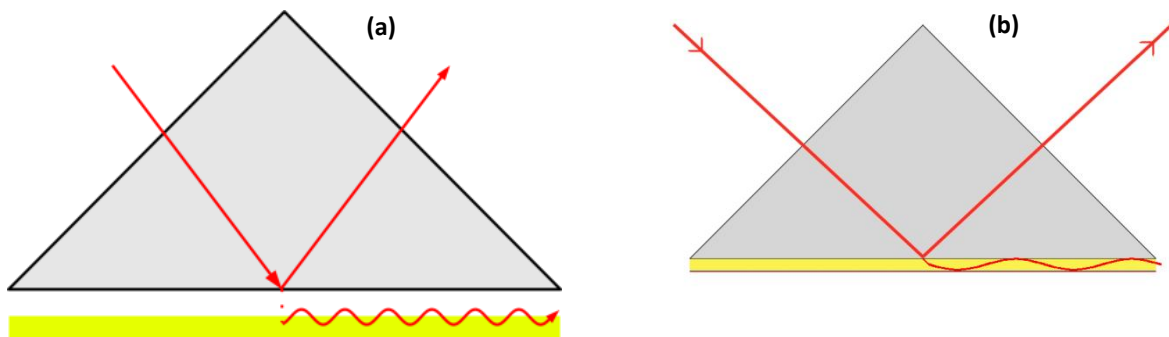

Fig 2: Excitation of Surface Plasmon Polaritons; (a) Otto configuration, (b) Kretschmann configuration

In Otto configuration, light is totally internally reflected from the prism surface. A thin metal film(e.g. gold) is then placed close enough to the prism wall so that the evanescent waves can interact with the plasma waves and excite the plasmons. In Kretschmann configuration, the metal film is evaporated on the glass prism itself. The evanescent waves then penetrate through the film and excite plasmons on the outer surface.

4.3 Instrumentation

In our lab we utilize a dove prism to achieve Kretschmann configuration. As one can see in the setup(fig 3) We place a glass slide on which a ~45nm layer of gold is coated using......We also put index matching oil between the prism and the glass slide so that the
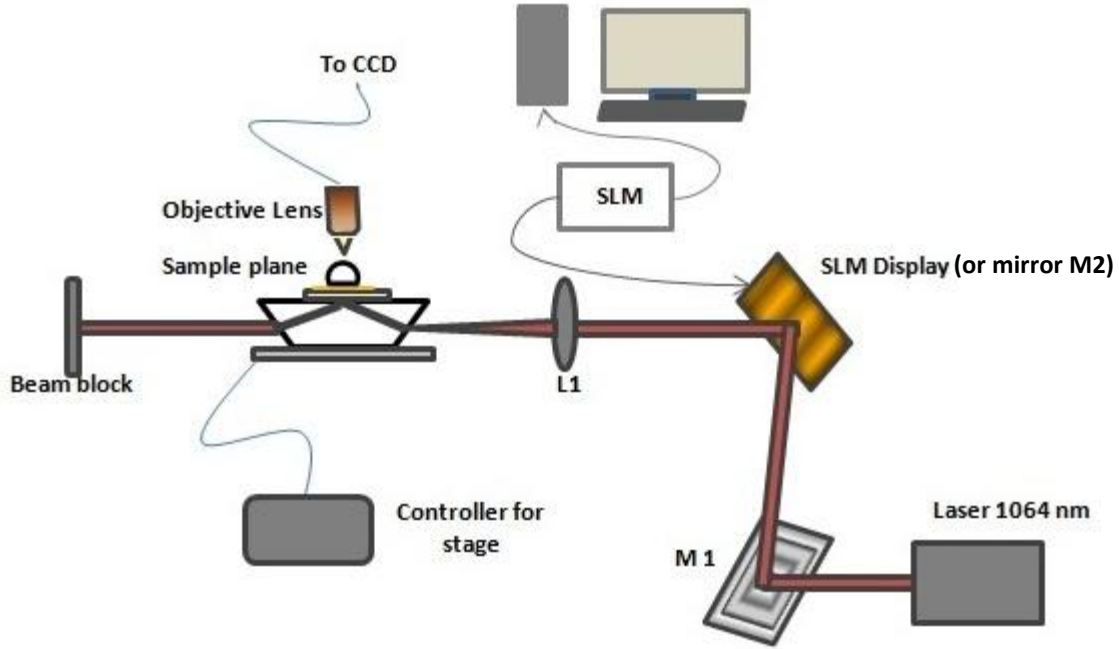
Fig 3: Setup for plasmon based IR trapping; SLM here is interchangeable with a second mirror M2

evanescent waves generated by the total internal reflection can leak into the glass slide and excite SPPs on the other side. We use a 1064nm laser of maximum power 2W for the experiment. We place a water based solution of 3μm silica beads on top of the glass slide and image our sample through 4x and 10x objectives to view the aggregate formation. The lens is being used to focus the laser on a certain spot on the inside surface of the prism. Although this experiment was done with a simple mirror, an SLM could be used instead as a modification. This will be discussed later.

4.4 Results and Discussion

We focus a 1064nm p-polarized laser onto the inner surface of the dove prism to cause total internal reflection. As and when the angle of this reflection matches the angle of plasmon resonance, SPPs are excited on the outer side of the gold film. Now this Plasmon propagation does two things. The first is it leads to plasmonic heating since we are using an infra-red laser which causes a convection current in the fluid medium cycling and stirring the micro-particles in addition to the usual Brownian force. The second is creation of a potential well which is suitable to trap the particles once they come near the point of incidence.

We can see from the images the formation of aggregates of these microspheres at the spot of TIR. This is due to those particles falling in that plasmonic potential well and

getting trapped. In a video taken from the CCD on can clearly see the movement of particles from all directions towards the point of laser incidence overcoming the Brownian motion. Once the laser is left on for a period of time, one can see the aggregate of particles forming at that point. Some snapshots taken by a 4x objective are shown below.
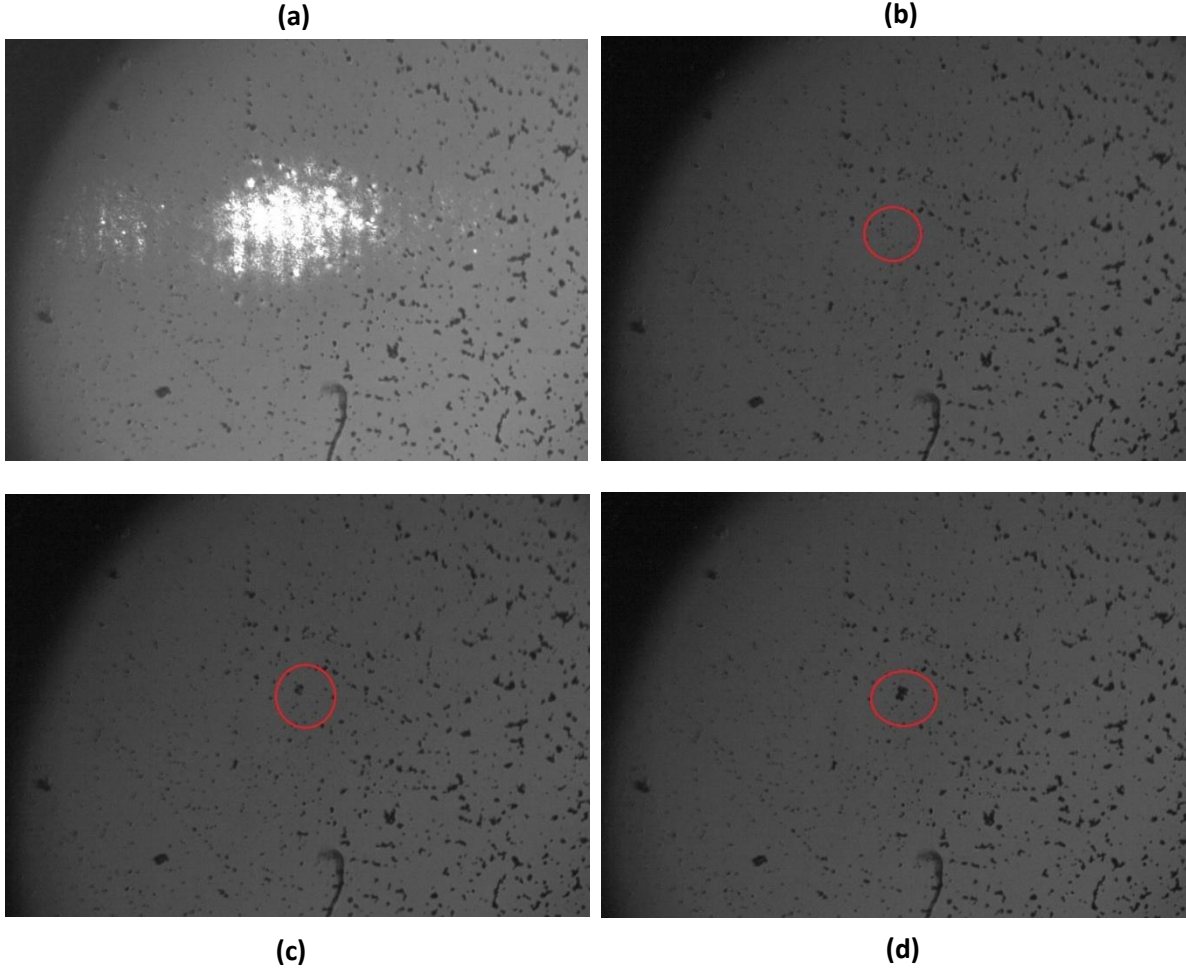

Fig 4: (a) Incident spot of laser without using a filter in fron of CCD; (b,c,d,) Formation of aggregate in the encircled area; Images in (b,c,d) by 4x objective and separated in time steps of 5 minutes

One can observe the growing number of particles in the trap region(encircled red) in steps of five minutes in time. To see the aggregate formation more clearly we shift to a 10x objective as well. In that case another interesting observation is made(fig 5). If we block the laser, the particles start dispersing from these aggregates to resume random motion and come back in the trap region after unblocking the laser. This proves that the trapping is due to plasmonic potential only and not a result of some other factors.

Also once can move the position of these aggregates by careful steering of the stage or the mirror. In figure 6, we observe the slight leftward movement of the bunch of trapped

particles on carefully steering the mirror placed just before the converging lens. Thus, we have also achieved mobility of this aggregate of microspheres. However, the trap was very sensitive to movement and freewheeling mobility in all directions seemed hard to achieve. More work is needed to be done in this regard.

(a)

(b)

(c)
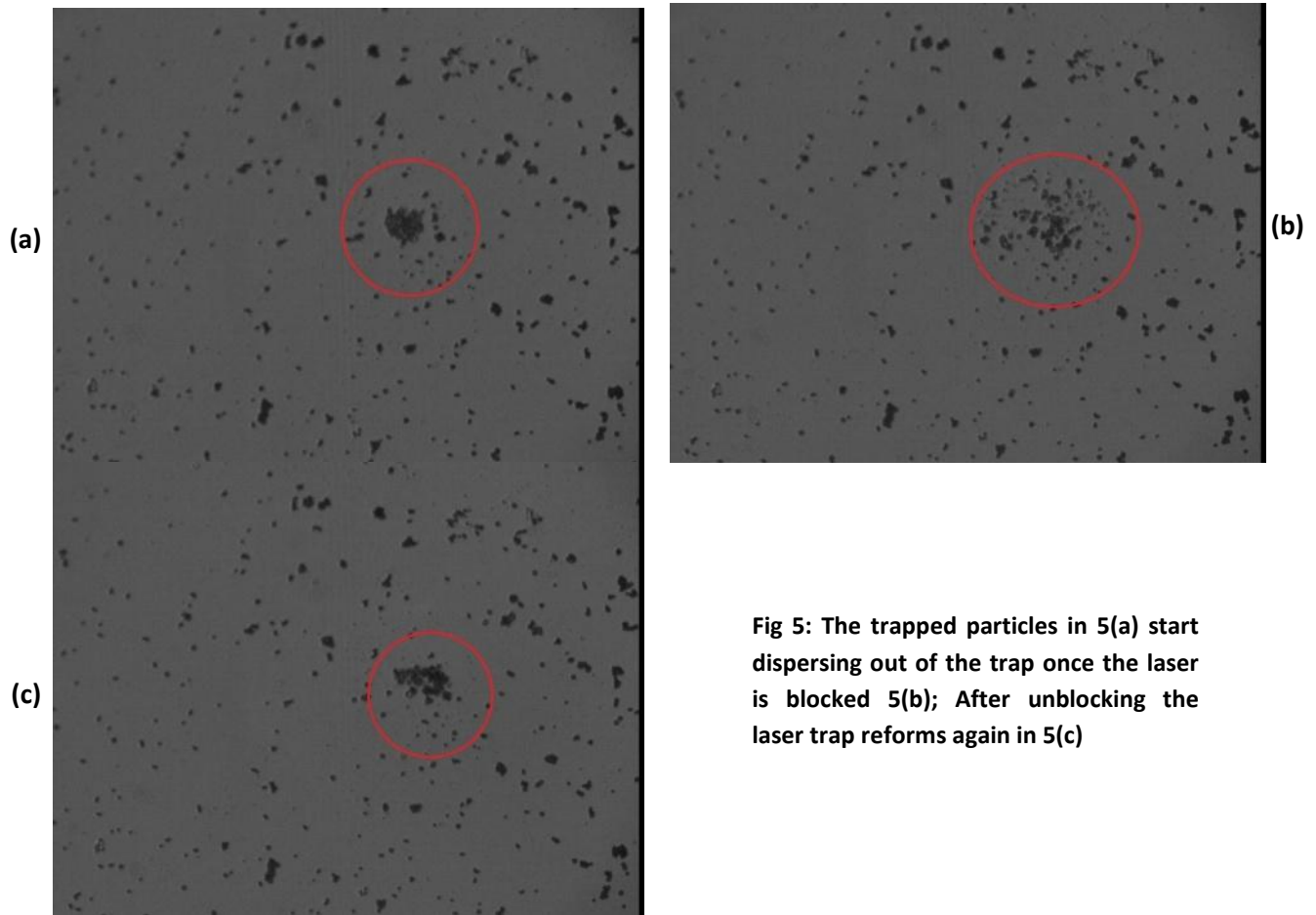
Fig 5: The trapped particles in 5(a) start dispersing out of the trap once the laser is blocked 5(b); After unblocking the laser trap reforms again in 5(c)

(a)

(b)
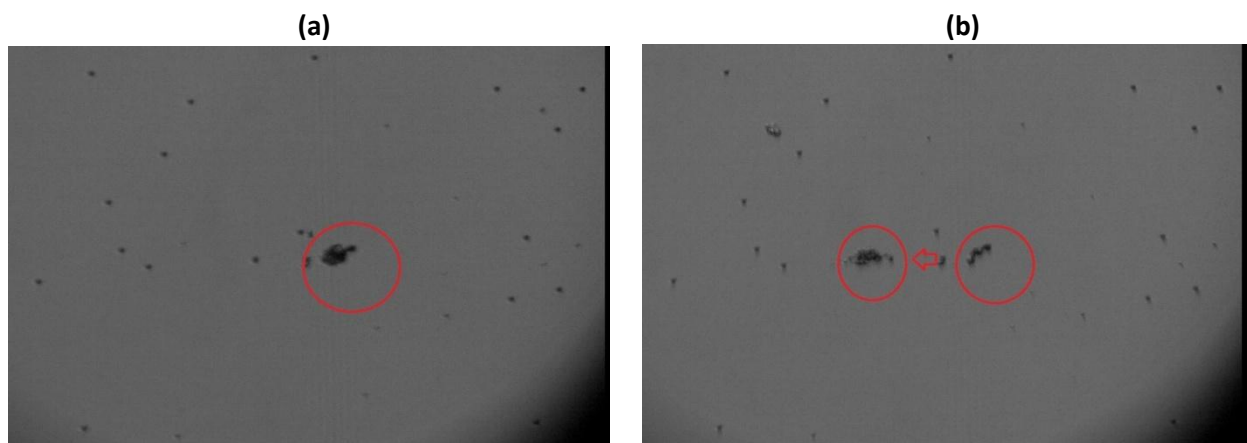
Fig 6: In (b) the laser is being steered using the kinematic mirror mount and shifting in trap position can be observed; Concentration of spheres decreased for clarity

4.5 Future Direction

In the coming weeks our aim will be to probe the behavior of these traps under structured light fields. The SLM that we introduced in the beam path as a modification plays an important part here. Through this we can introduce modified light fields in the same setup. Our main concern will be investigating the properties or points of dissent of the trap under Bessel beam illumination. Since we've already been able to demonstrate a stable Bessel beam earlier, it will be easier to incorporate in this case. However there is no reason why we cannot go ahead with other forms of structured light in the experiment as well. This will give us a better insight into the nature of these plasmonic traps and enable us to characterize them on the basis of many different incident light fields.

We also plan to create normal optical traps with structured light fields e.g. Bessel beams. In this case we can utilize many of the advantages which such fields provide in the kind of optical traps they create. These include axial multi-particle trapping, transferring angular momentum of higher Laguerre-Gaussian modes and other similar experiments which can prove helpful in numerous applications in our lab. Another interesting area of research is illuminating nanostructures with these structured fields and observing the emissions in back-focal plane or k-space. This gives us valuable information about directivity etc. More about Fourier space imaging is discussed in Appendix A.

Appendix A

FOURIER PLANE IMAGING

Information about how plasmonic and metamaterial substrates scatter light into the far field[39,40,41] is of prime importance in the field of plasmonics. The distribution of light scattered in different directions is as useful as the absorption, scattering and extinction cross- section data. We are thus faced with a problem of determining this angular distribution since scattering signals from these nanostructures are very weak and hard to collect. Such measurements have been done using arrays of nanostructures which leads to strengthening the signals. The problem however is that these arrays have structure factors like grating orders and speckles which renders collecting information about individual scatterers impossible. To overcome such effects Fourier pane imaging or back focal plane imaging has been used in recent research experiments.

This technique relies on the fact that microscope objectives can not only be used for imaging purposes but also to get directional information about scatterings and emissions. Light radiated by a single nanostructure can be collected using a high NA objective and the back aperture in this case contains vital information about k-space of the electromagnetic fields. This information can be retrieved by a method called Back Focal Plane(BFP) imaging.

Concept

In any imaging setup for example in a microscope, there is a whole optical train setup to do the task. This includes elements illumination, condenser, sample plane, imaging elements etc. Such varied elements can actually be grouped into two sets of conjugate planes. The first set of conjugate planes contains information about real space along the whole optical train. Our image which we see in the microscope is one of these first set of planes. The second set however contains information about the momentum space or Fourier space. If we can employ a technique which harnesses this information, we can get data about the k-space or directionality. For example emitters at different locations on an x-y plane which emit in the same direction will all correspond to one point in this momentum space. The figure on the next page enlisting all such planes in an imaging setup will make the picture more clear. All the planes labeled in red are real space planes including the image plane and all the planes labeled in blue are Fourier space planes which includes back aperture of the objective.
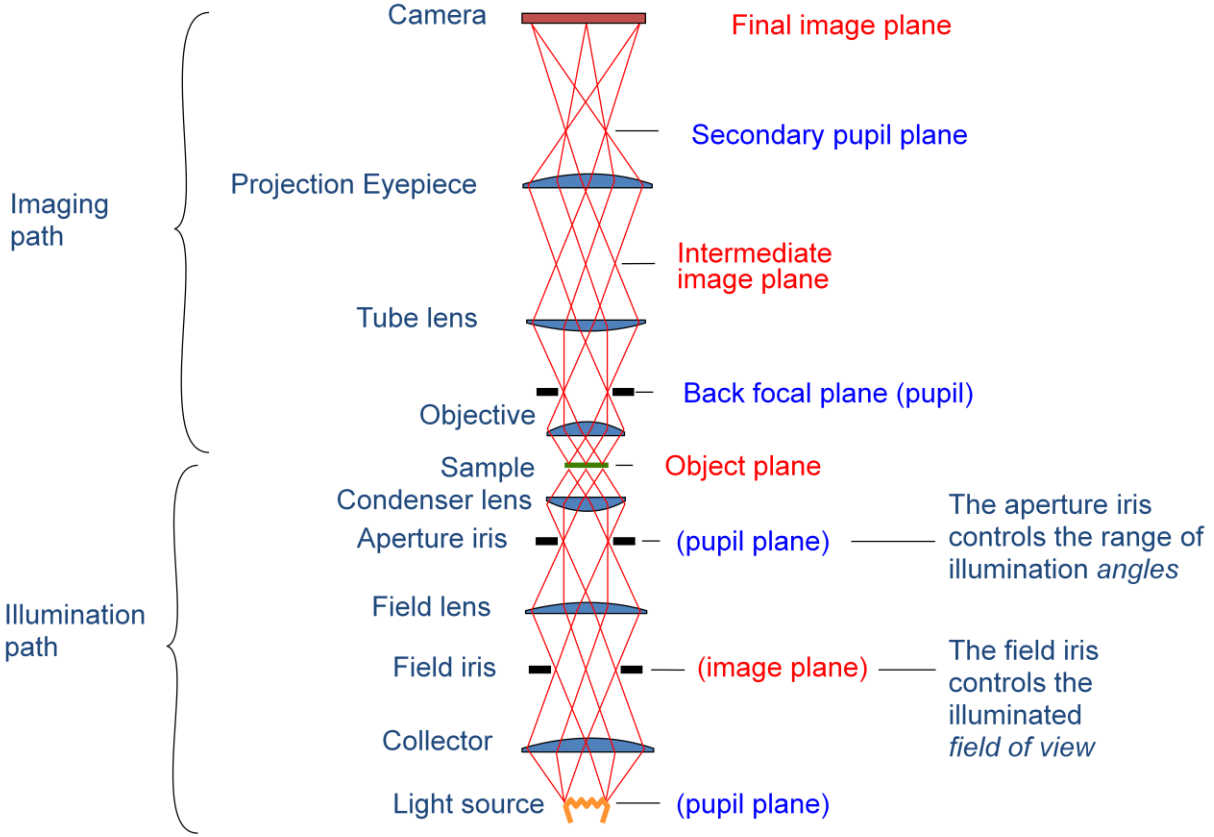
Fig 1: Different planes in an imaging setup

Therefore if we are able to project the back aperture of the objective onto a suitable screen(e.g. a CCD camera) we can successfully retrieve this k-space data. This is exactly what the BFP imaging deals with. The back aperture of a high NA objective used for illumination as well as collection of scattered light from nanostructures is projected onto a CCD using suitable optics. The next section gives a brief about the design considerations of such a setup.

Instrumentation

We use a commercial inverted microscope(Olympus IX371) as our platform and modify the optics accordingly. A 633nm He-Ne laser is used for illumination and we collect the back scattered light using a high numerical aperture oil immersion objective lens(Nikon UPlan FL; NA= 1.3). This scattered light is then taken out of one of the exit ports. The lenses L1(inside the microscope) and L2 in the setup shown form a 4f telescopic arrangement. The diaphragm in between these lenses is used for spatial filtering i.e. selecting certain areas from the field of view which we want to capture. The tube lens is for focusing the image on CCD. The main function is performed by a short focal length
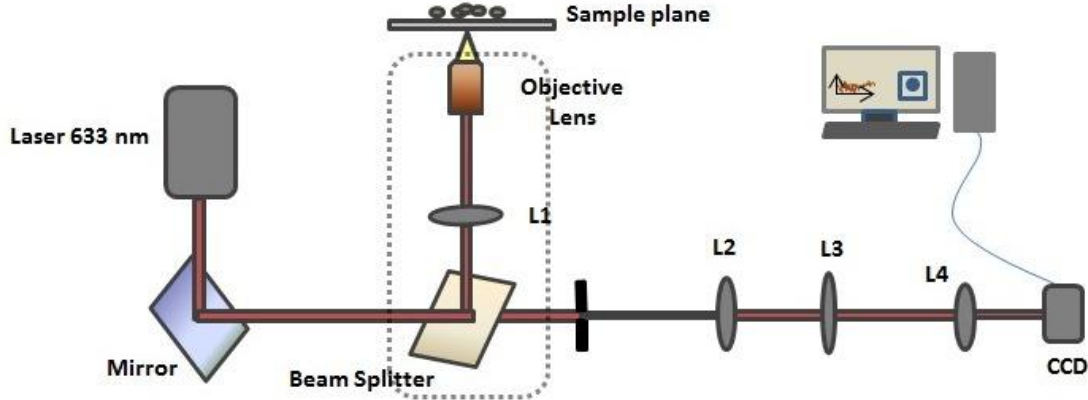
Fig 2: Setup for Fourier plane imaging; L1,L2 – 4f arrangement(f=150mm); L3 - tube lens(f=150mm); L4 – Bertrand Lens(f=60mm)

Bertrand lens which is placed on a flippable lens mount. As we know a lens inherently gives a Fourier transform of the light on the other side's focus. Thus, the Bertrand lens focuses the back aperture of the objective on to the CCD and we can retrieve important direction information on single structure emissions.

Results

To present an example of how this technique works out, here are some images of a propagating SPP mode in a silver nanowire.
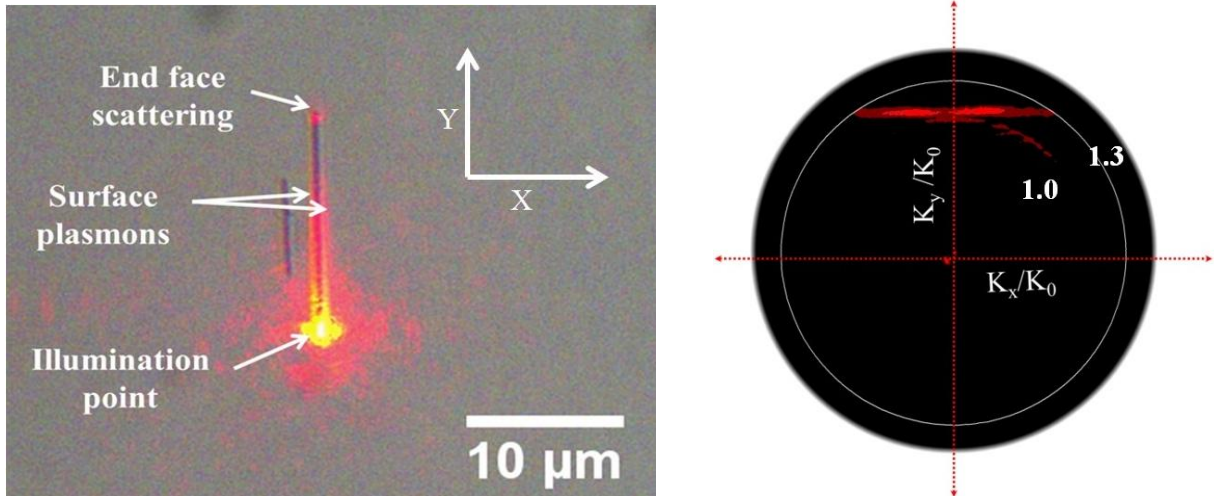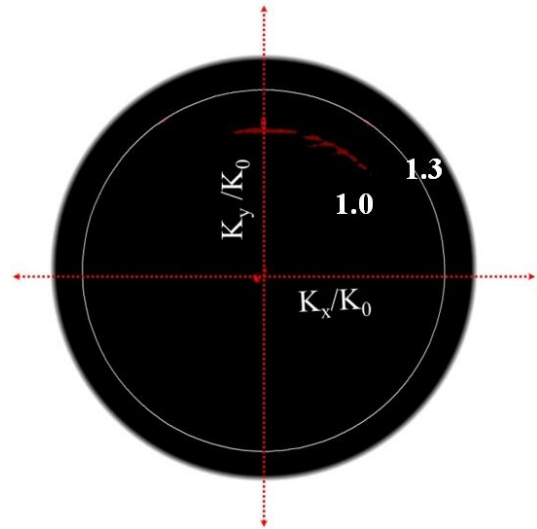

Fig 3: (a) Propagation of an SPP mode in Ag nanowire; (b) k-space image of the guided mode

The Ag NW used were nm in diameter and about μm long. In the first image one can see the light incident on one of the ends of the nanowire which excites an SPP mode. This propagates over the length of the wire and at the end which can also be treated as a defect, the surface plasmons couple to emit light in the far field. The second image shows the same phenomena in the k-space or Fourier plane. Once we flip the Bertrand lens into position we can observe that there is confinement of the propagating plasmons in k_x direction and propagating guided mode can be seen in k_y direction. Thus on can get important directional data about these propagating modes.

To go a step further we use our spatial filter to select only the end of the wire which is emitting light in the far field. In its Fourier plane image, one can observe an arc in the direction of emission. These arcs correspond to specific angles in the real x-y plane. Therefore we can determine in which direction the emission takes place.

Fig 4: Fourier plane image with only the point of emission from the nanowire selected

Besides this data shown here as an example, there are numerous other applications of this imaging setup and the ongoing experiments in our lab use it in many different ways.

References

1. **A. Stern, R.A. Farell.** 1960, Phys. Rev. 120, p. 130.

2. **Ritchie, R.H.** 1957, Phys. Rev. 106, p. 874.

3. **Ashkin, A.** s.l. : Phys. Rev. Lett., 1970, Vol. 24, p. 156.

4. *A preliminary communication on the pressure of heat and light radiation.* **E.F. Nicholes, G.F. Hull.** 1901, Phys. Rev., Vol. 13, pp. 307-320.

5. *Experimental examination of light pressure.* **Lebedev, P.N.** 1901, Ann. Phys., Vol. 6, pp. 433-458.

6. **Economou, E.N.** 1969, Phys. Rev., Vol. 182, p. 539.

7. **Ritchie, R.H.** 1973, Surf. Sci., Vol. 34, p. 1.

8. **T.W. Ebbeson, H.J. Leztec, H.F. Ghaemi, T.Thio, P.A. Wolff.** London : s.n., 1998, Nature, Vol. 391, p. 667.

9. **J. Takahara, S. Yamagishi, H. Taki, A. Morimoto, T. Kobayashi.** 1997, Opt. Lett., Vol. 22, p. 475.

10. **K. Tanaka, M. Tanaka.** 2003, App. Phys. Lett., Vol. 82.

11. **A. Brecht, G. Gauglitz.** 1995, Biosens. Bioelectron., Vol. 10.

12. **A.J. Hayes, R.P.V. Duyne.** 124, 2002, Jour. Am. Chem. Soc., Vol. 10.

13. **Maier, Stefan A.** *Plasmonics : Fundamentals and Applications.* University of Bath : Centre for Photonics and Photonics Materials, 2007.

14. **Zhipeng Li, Kui Bao, Yurui Fang, Yingzhou Huang, Peter Nordlander, Hongxing Xu.** 2010, Nano Lett., Vol. 10, pp. 1831-1835.

15. **Yaoguang Ma, Xiyuan Li, Huakang Yu, Limin Tong, Ying Gu, Qihuan Gong.** 8, April 15, 2010, Optics Letters, Vol. 10.

16. **H. Ditlbacher, A. Hohenau, D. Wagner, U. Kreibig, M. Rogers.** 2005, Phys. Rev. Lett., Vol. 95.

17. **A.W. Sanders, D.A. Routenburg, B.J. Wiley, Y.N. Xia, M.A. Reed.** 2006, Nano Lett., Vol. 6, pp. 1822-1826.

18. **A.V. Akimov, A. Mukherjee, C.L. Yu, D.E. Chang, A.S. Zibrov, M.D. Lukin.** 2007, Nature, Vol. 450, pp. 402-406.

19. **M.W. Knight, N.K. Grady, R. Bardhan, F. Hao, P. Nordlander, N. Halas.** 2007, Nano Lett., Vol. 7, pp. 2346-2350.

20. **A. Ashkin, J.M. Dziedzic.** 1971, Appl. Phys. Lett., Vol. 19, p. 283.

21. **al., A. Ashkin et.** 1986, Opt. Lett., Vol. 11, p. 288.

22. **Ashkin, A.** 2000, IEEE Jour. Sel. Top. Quantum Electron, Vol. 6, p. 841.

23. **H. Misawa, K. Sasaki, M. Koshioka, N. Kitamura, H. Masuhara.** 1992, Appl. Phys. Lett., Vol. 60, pp. 310-312.

24. **K. Sasaki, M. Koshioka, H. Misawa, N. Kitamura.** 1991, Opt. Lett., Vol. 16, pp. 1463-1465.

25. **K. Visscher, G. Brakenhoff, J. Krol.** 1993, Cytometry, Vol. 14, pp. 105-114.

26. **K. Visscher, S. Block, S. Gross.** 1996, IEEE Jour. Sel. Top. Quantum Electron, Vol. 2, pp. 1066-1076.

27. **J. Curtis, B. Coss, D. Grier.** 2002, Opt. Comm., Vol. 207, pp. 169-175.

28. **Grier, D.** 2003, Nature, Vol. 424, pp. 810-816.

29. **Miles Padgett, Robert D. Leonardo.** 2011, Lab on a chip, Vol. 11, p. 1196.

30. **Christian Maurer, Stefan Bernet, Monika Ritsch-Marte.** 1, 2011, Laser Photonics Rev., Vol. 5, pp. 81-101.

31. **Durnin, J.** 1987, Jour. Opt. Soc. of Am. A , Vol. 4, pp. 651-654.

32. **J. Durnin, J.J. Miceli, J.H. Eberly.** 1987, Phy. Rev. Lett., Vol. 56, p. 2611.

33. *Bessel Beams : Diffraction in a new Light.* **D. McGloin, K. Dholakia.** 1, 2005, Contemporary Physics, Vol. 6, pp. 15-28.

34. **Indebetouw, G.** 1989, Jour. Opt. Soc. Am. A, Vol. 6, pp. 150-152.

35. **A. Vasara, J. Turunen, A.T. Friberg.** 1989, Jour. Opt. Soc. Am. A, Vol. 6, p. 1748.

36. *Extended organization of colloidal microparticles by SPP excitation.* **al., V. Garcez-Chavez et.** 2006, Phys. Rev. B, Vol. 73, p. 085417.

37. *Surface plasmon radiation forces.* **G. Volpe, R. Quidant, G. Badenes, D. Petrov.** 2006, Phys. Rev. Lett., Vol. 96, p. 238101.

38. *Plasmon nano-optical tweezers.* **Matheiu L. Juan, Maurizio Righini, Romain Quidant.** 2011, Nature photonics , Vol. 56.

39. **Abajo, F. J. Garcia de.** 2007, Rev. Mod. Phys., Vol. 79, p. 1267.

40. **I Sersic, M Frimmer, E Verhagen, A F Koenderink.** 2009, Phys. Rev. Lett., Vol. 103, p. 213902.

41. **A Pors, M Willatzen, O Albrektsen, S I Bozhevolnyi.** 2010, Jour. Opt. Soc. Am. B, Vol. 27, p. 1680.

42. **J. Durnin, J. J. Micelli Jr., J. H. Eberly.** 2, 1988, Optics Letters, Vol. 13, pp. 79-80.

43. **Ivana Sersic, Christelle Tuambilangana, A Femius Koenderink.** 2011, New Journal of Physics, Vol. 13, p. 083019.

44. **Oriane Mollet, Serge Huant, Aureleian Drezet.** 27, 2012, Optics Express, Vol. 20, p. 28923.